Article:

Smith, C.C. and Tatari, A. (2016) Limit analysis of reinforced embankments on soft soil. Geotextiles and Geomembranes, 44 (4). pp. 504-514. ISSN: 0266-1144

https://doi.org/10.1016/j.geotexmem.2016.01.008

Limit Analysis of Reinforced Embankments on Soft Soil

Colin C Smith[a,*], Alireza Tatari[a]

[a] *Department of Civil and Structural Engineering, The University of Sheffield, Mappin Street, Sheffield, S1 3JD, UK*

Abstract

Previous research into the stability of reinforced embankments founded on soft soil has presented limited studies based on a narrow range of assumed failure mechanisms. In this paper comprehensive parametric studies of reinforced and unreinforced embankments were conducted using the general purpose computational limit analysis approach Discontinuity Layout Optimization (DLO). Comparisons with previous Limit Equilibrium and FE results in the literature showed good agreement, with the DLO analysis generally able to determine more critical failure mechanisms. Simplified, summary design envelopes are presented that allow critical heights and reinforcement strengths to be rapidly determined based on soft soil strength and depth, and shows how the balance between soft soil strength and reinforcement strength combines to affect overall stability.

Keywords: Geosynthetics, discontinuity layout optimization, limit analysis, failure, reinforcement, safety factor.

1. Introduction

The use of a basal geosynthetic reinforcement for an embankment constructed on soft soils can significantly enhance stability and allow construction to heights substantially higher than could be achieved without reinforcement (Rowe and Soderman, 1987). Two common analysis methods used by geotechnical engineers to check the stability of embankments over soft soil are (i) conventional limit equilibrium such as Coulomb wedge or the method of slices and (ii) the finite element (FE) method. The general concept of the former method is to find the most critical slip surface with the lowest factor of safety. This may be defined as the shear strength of the soil divided by shear stress required for equilibrium, Duncan (1996).

*Corresponding author Tel: +44 114 2225717
Email addresses: c.c.smith@sheffield.ac.uk (Colin C Smith), a.tatari@sheffield.ac.uk (Alireza Tatari)

Most limit equilibrium methods indirectly model the reinforcement as a single representative force which acts at the intersection between the reinforcement and the failure mechanism. The failure mechanism may be modelled as a slip-circle using the method of slices (e.g. Rowe and Soderman (1985), Hird (1986), Sabhahit et al. (1994)), or as a log-spiral (e.g. Leshchinsky (1987), Leshchinsky and Smith (1989)) or using a translational mechanism (e.g. Jewell (1988)).

While limit equilibrium is simple and straightforward it makes an assumption about the nature of the failure mechanism which can lead to inaccuracy. In contrast FE methods can accurately model both working conditions and failure modes, representing the reinforcement as a structural membrane with an axial stiffness and negligible flexural rigidity. More recent work in the literature has focused on this method *e.g.* Rowe and Soderman (1985); Rowe and Soderman (1987); Duncan and Schaefer (1988); Hird and Kwok (1989); Hird et al. (1990); Chai and Bergado (1993); Rowe and Hinchberger (1998); Rowe and Li (2005) and Zhang et al. (2015). However, modelling the embankment problem by finite elements typically requires significant time and is more complex with regard to choosing the problem parameters in comparison with limit equilibrium methods (Duncan, 1996).

Recently the advent of numerical direct methods has allowed the rapid solution of limit analysis problems in a fully general way. These provide a middle way between the simplification in limit equilibrium analysis and the relative complexity of the FE method. An elasto-plastic analysis typically requires many increments in order to find the critical factor of safety in contrast to a computational limit analysis approach which can directly determine the collapse state through optimization. One of the main advantages of limit analysis over FE methods is it requires only two strength parameters for any material modelled: the cohesion, c' or c_u, and the angle of shearing resistance, ϕ', of the soil. Computational limit analysis approaches have been recently used to analysis a range of reinforced soil problems *e.g.* Leshchinsky et al. (2012), Clarke et al. (2013) and Vahedifard et al. (2014). These papers utilise the Discontinuity Layout Optimization method (Smith and Gilbert, 2007), which is adopted in this paper to undertake a parametric study of embankment stability.

The aim of this paper is to illustrate how reinforced embankments can be modelled in limit analysis; to investigate the range of failure modes that can occur and to produce a series of non-dimensional design charts for different geometries of embankment which allows the necessary minimum embankment soil strength and reinforcement strength required for stability to be determined in terms of the embankment geometry, base soil strength, soil/geotextile interface coefficient and surcharge. This provides a significantly more comprehensive set of charts compared to previous works that have utilised Limit Equilibrium such as Leshchinsky and Smith (1989), Duncan et al. (1987), Leshchinsky (1987) and Hird (1986) without using an analysis which typically adopts only one mode of failure.

2. Mechanics of reinforced embankments

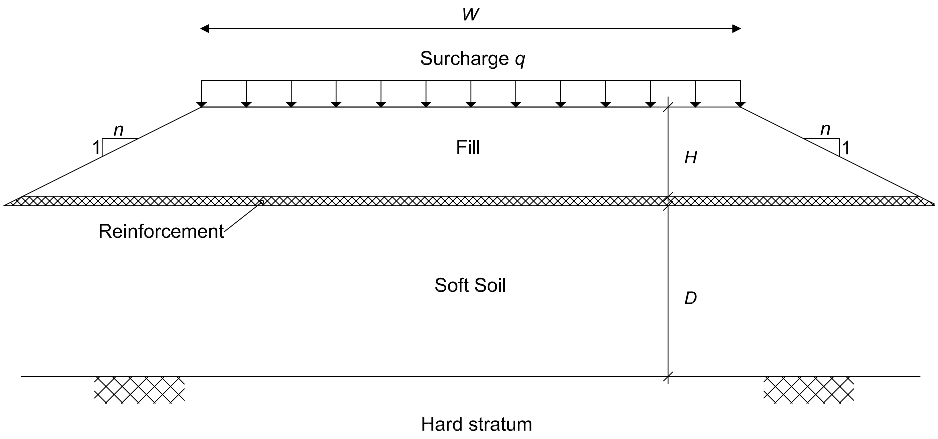

Figure 1: geometry of embankment model

Manceau et al. (2012) recommend three ULS states should be considered as follows: (i) deep-seated failure, (ii) lateral sliding (iii) extrusion. While deep seated failure requires an analysis such as method of slices or equivalent, the latter two mechanisms can be analysed relatively simply using limit equilibrium. Jewell (1988), presented simple analytical equations based on force equilibrium for the analysis of reinforced and unreinforced embankments of geometry depicted in Figure 1 and described by the parameters listed in Table 1 (in the analysis $c' = 0$ was assumed). These provide useful equations for calibration and a conceptual model of two of the main mechanisms of collapse.

In Figure 2a, the reinforcement provides resistance against lateral failure of the embankment itself with friction on the upper reinforcement surface of $\alpha_s \tan\phi'$ where α_s is the reinforcement interface coefficient. Equilibrium analysis gives the following required side slope gradient n for stability:

$$n > \frac{K_a}{\alpha_s \tan\phi'}(1 + \frac{2q}{\gamma H}) \tag{1}$$

where the design value of active earth pressure coefficient, $K_a = \frac{1-\sin\phi}{1+\sin\phi}$.

In Figure 2b the reinforcement provides shear resistance against lateral squeezing of the soft soil beneath the embankment. Equilibrium analysis of the deep failure mechanism gives the factor of safety F_s on the soft soil strength as follows:

$$F_s = \frac{c_u}{q + \gamma H}(4 + (1 + \alpha_c)\frac{nH}{D}) \tag{2}$$

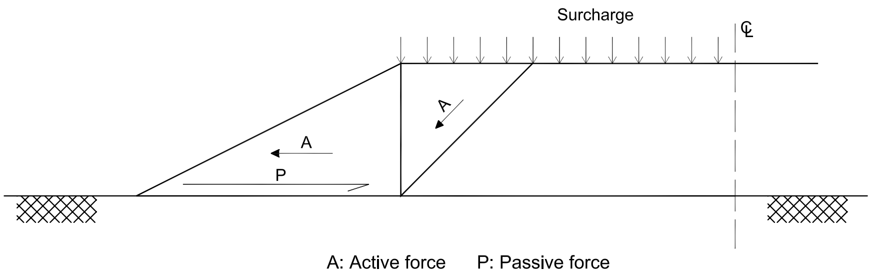

(a) Lateral sliding

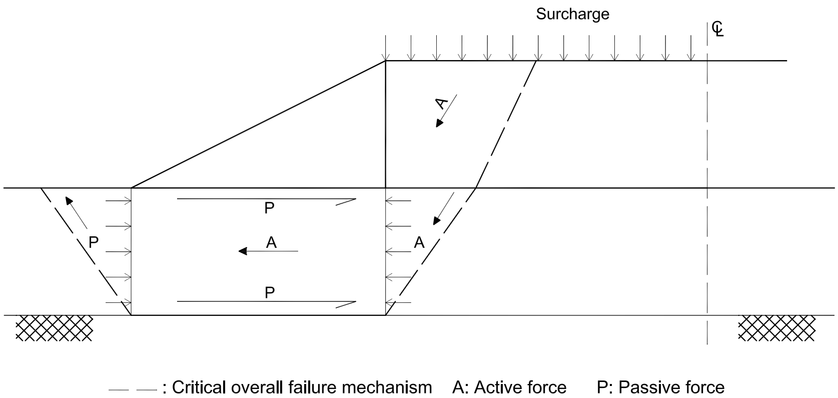

(b) Extrusion

Figure 2: The mechanism of failure of embankment over soft soil (after Jewell, 1996)

Table 1: Reinforced embankment analysis parameters

Symbol	**Definition**
c'	cohesion of the soil of embankment fill
ϕ'	friction angle of soil of embankment fill
γ	unit weight of soil of embankment fill
c_u	shear strength of soft soil
R	rupture strength of reinforcement per unit width
H	height of embankment
W	width of top of embankment
D	thickness of soft soil
q	surcharge
n	side slope gradient $(nH : 1V)$
α_c	interface coefficient between reinforcement and soft soil
α_s	interface coefficient between reinforcement and embankment fill

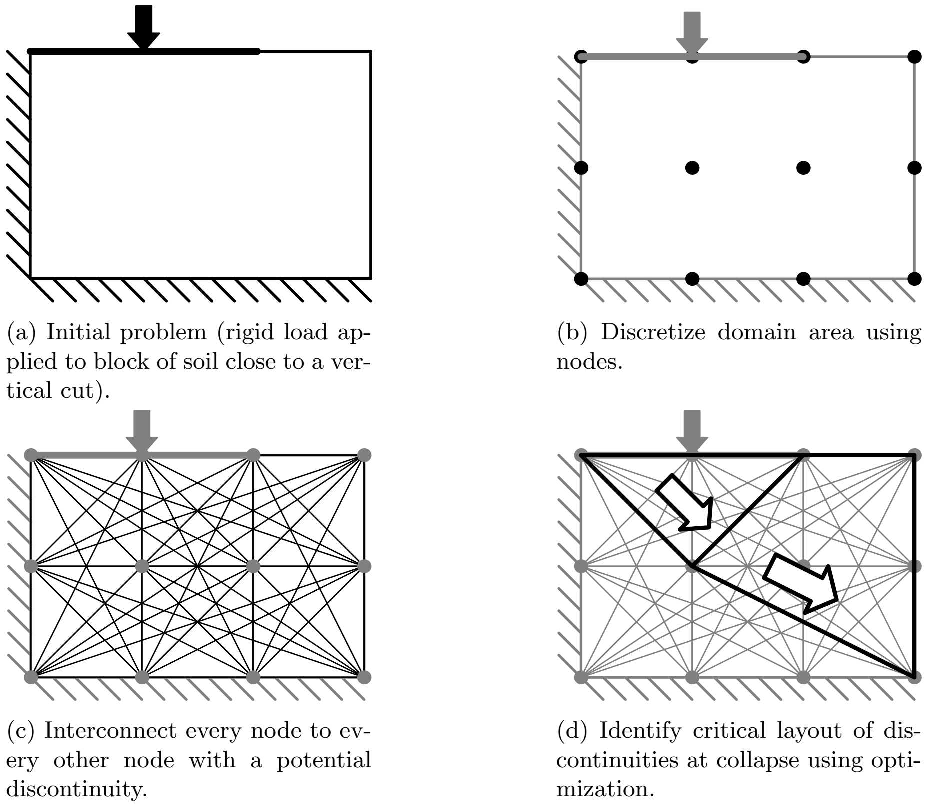

(a) Initial problem (rigid load applied to block of soil close to a vertical cut).

(b) Discretize domain area using nodes.

(c) Interconnect every node to every other node with a potential discontinuity.

(d) Identify critical layout of discontinuities at collapse using optimization.

Figure 3: Stages in DLO solution procedure (after Gilbert et al. (2010)).

The minimum force R within the reinforcement required to provide the stability for the failure mechanism in Figure 2b is given by equation 3:

$$R = \gamma H^2 \left(\frac{\alpha n D}{4D + (1+\alpha) n H} + \frac{K_a}{2} \right) \tag{3}$$

Jewell also presented the following equation for checking the stability of an unreinforced embankment (the failure mechanism is not present here):

$$F_s = \frac{c_u}{\gamma H} \left(\frac{8D + 2nH}{2D + K_a} \right) \tag{4}$$

Such limit equilibrium equations have the value of simplicity and clarity but it is not necessarily clear whether these are conservative or non-conservative in all cases.

3. Discontinuity layout optimisation (DLO)

3.1. Geotechnical analysis

Discontinuity layout optimization is a computational limit analysis method which is able to identify the critical failure mechanism and collapse load for any geotechnical stability problem. Examples of this analysis approach applied to soil only problems (with no reinforcement) may be found in Smith and Gilbert (2007, 2013) and Leshchinsky (2015). Figure 3 illustrates the stages in the DLO procedure for finding the layout of sliplines that form the critical collapse mechanism (after Gilbert et al. 2010). The accuracy of the method depends on the number n nodes employed which allow the critical mechanism to be selected out of a set of $n(n-1)/2$ potential sliplines. Using the principles of duality, the DLO formulation may be presented in either a kinematic energy form or an equilibrium and yield form.

3.2. Modelling reinforcement in DLO

Reinforcement is modelled as a one dimensional element similar to that described by Clarke et al. (2013). This element is able to model failure in bending, tensile rupture and compressive failure controlled by parameters M_p, R, and C respectively, where M_p is the plastic moment of resistance and C is the compressive strength of the reinforcement. The element described by Clarke et al. (2013) was designed also to allow the modeling of soil nails and so had the additional ability to allow soil to 'flow around' the element controlled by a lateral and pullout resistance. In this paper these properties were not required and these resistances were set to ∞.

Each engineered element has three parallel components (as shown in Figure 4) which comprise: an upper boundary interface, the reinforcement itself and a lower boundary interface. For the purposes of modelling geotextile reinforcement M_p is set to zero to allow free flexure, C is set to zero and the upper and lower boundaries are modelled with Mohr-Coulomb materials with strength $\alpha_s \tan \phi'$ and $\alpha_c c_u$ respectively.

In the equilibrium formulation of DLO, for each discrete element i of the reinforcement, variables are assigned to represent the shear stress $\tau_{u,i}, \tau_{l,i}$, on the upper and lower faces respectively, and the tensile force T_i and bending moment M_i in the reinforcement. The set of τ_u, τ_l, M, T are found that give the maximum load on the system that does not violate the following constraints:

1. $\tau_l \leq \alpha_c c_u$
2. $\tau_u \leq \alpha_s(c' + \sigma'_n \tan\phi')$
3. $C \leq T \leq R$
4. $M \leq M_p$

where σ'_n is the effective normal stress acting on the reinforcement.

It is noted that even if $M_p = R = C = 0$, the modelled reinforcement will still affect the mechanics of the system in that shear displacements are not permitted directly through the reinforcement element. However this can be represented via element rotations. With sufficiently small segments the same effect is achieved. Use of a higher nodal density along the reinforcement can therefore be beneficial in some cases.

Note that in a limit analysis formulation such as DLO, yield or rupture of the reinforcement does not lead to breakage or fracture but to unrestricted ductile elongation that still allows transmission of tensile forces along the length of the reinforcement.

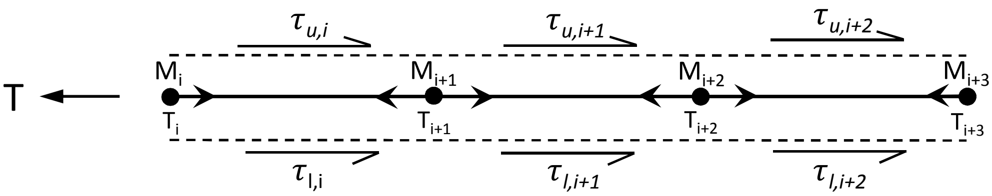

Figure 4: Modelling flexible reinforcement in DLO for segment or node i, τ_u: upper boundary soil/reinforcement interface stress (kPa), τ_l: lower boundary soil/reinforcement interface stress (kPa), T: tensile force in reinforcement (kN, per m width), M: bending moment in reinforcement (kN, per m width).

4. Embankment modelling

4.1. Numerical model

Analysis was carried out using the implementation of DLO within the software LimitState:GEO Version 3.2a (LimitState, 2014). In the model, the boundary nodal spacing was set to be half that within the internal solid bodies as is recommended (LimitState, 2014). A series of internal vertical boundaries were also modelled within the embankment to allow 'bending' (or 'snapping') failure of the embankment. A simple example of this is shown in Figure 5d. Selected models across the parameter space were evaluated using nodal spacings on a square grid of $H/1$ to $H/10$. Typical results are shown in Appendix A. Based on these an accuracy of 1-2% in terms of the factor of safety on soil strength would be achieved with a nodal spacing of $H/5$. This spacing was selected as a compromise between accuracy and speed.

4.2. Failure mechanisms

Four distinct mechanisms of failure were generated by the DLO analysis and are shown in Figure 5. These mechanisms can be described as follows:

(a) Lateral sliding failure (surface failure).
(b) Deep seated global failure.
(c) Lower layer failure (squeezing/extrusion failure) with sinking.
(d) Lower layer failure (squeezing/extrusion failure) with 'snapping'.

For a high strength lower stratum, failure is in the shoulders of the embankment only (Figure 5a). For low strength reinforcement the dominant failure mechanism is a deep seated global failure accompanied by yield of the reinforcement (Figure 5b). In this type of failure, significant shearing happens in the main body and side slopes of the embankment. For high strength reinforcement significant 'squeezing' deformation is primarily seen in the lower stratum. The embankment itself either undergoes very localised shearing and vertical 'sinking' translation (Figure 5c) or rotational 'snapping' (Figure 5d). The latter mechanism is more likely to occur and need not involve any significant deformation/yielding of the reinforcement which simply rotates. To the authors' knowledge, the latter type of failure has not been previously examined in the literature.

4.3. Verification

4.3.1. Translational failure mechanisms

To permit direct comparison between the analytical solutions of Jewell (1988) and the DLO method for the analysis of surface failure (equation 1 and figure 2a), a simplified constrained model was first set up in DLO, setting the boundaries of the model to coincide exactly with the mechanism geometry used by Jewell. The relevant soil properties were applied to these boundaries while the solid bodies between the boundaries were assigned a rigid material of the same unit weight as the soil. This ensures failure can only occur along the pre-defined boundary lines, thus forcing the mechanisms to match those of Jewell's. The results, given in Figure 6, show, as expected, that the constrained DLO analysis exactly matches the analytical solution (which can be regarded as an upper bound analysis) while the unconstrained DLO analysis, results also given in Figure 6, give more critical results.

Figure 7 illustrates the comparison between the results of DLO and equations 2 and 4 for deep seated failure of reinforced and unreinforced embankments respectively. The results of analyses show a good match. However the DLO results are not consistently more critical as might be expected. This can be

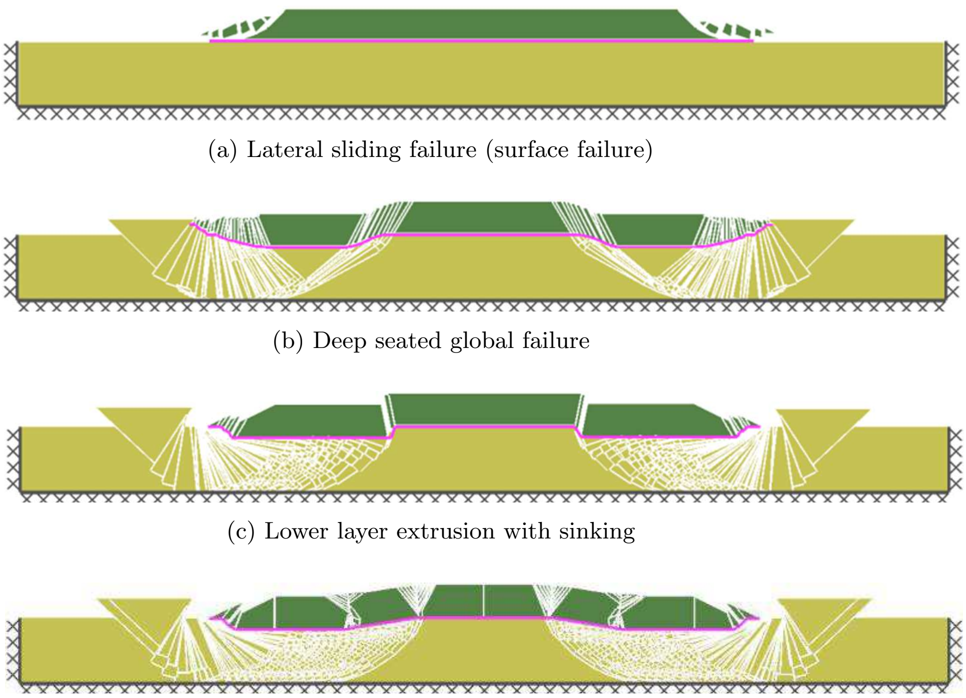

(a) Lateral sliding failure (surface failure)

(b) Deep seated global failure

(c) Lower layer extrusion with sinking

(d) Lower layer extrusion with 'snapping'

Figure 5: Failure mechanisms of embankment over soft soil (exaggerated)

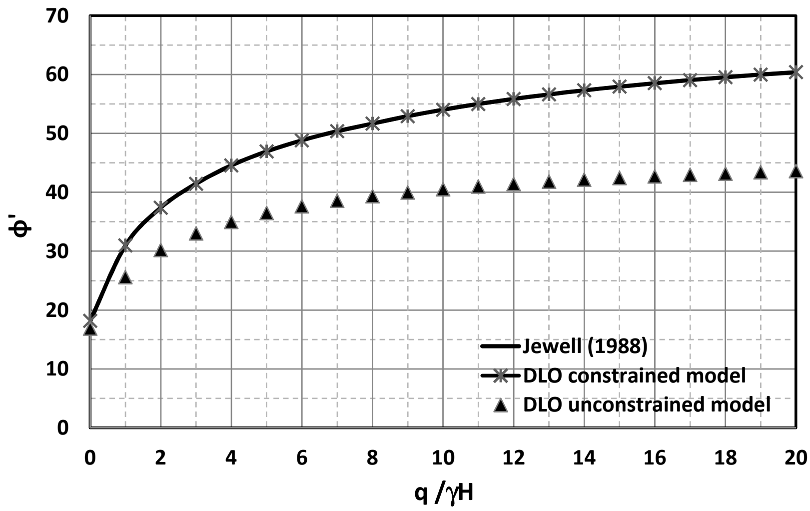

Figure 6: Plot of ϕ' required for factor of safety of 1.0 against $q/\gamma H$ for Jewell's analytical method (1988) and the current approach ($n = 2$ and $\alpha_s = 0.8$).

attributed to the form of the analytical equations which are based on limit equilibrium rather than limit analysis and, while probably not adopting an optimal mechanism, do neglect soil strength in various parts of the system.

4.3.2. Rotational mechanisms

Leshchinsky and Smith (1989) used an upper bound log-spiral rotational analysis for checking the factor of safety of an unreinforced embankment constructed on soft clay. The results were expressed in terms of a stability number:

$$N_m = \frac{1}{\gamma H} \frac{c_u}{F_s} \tag{5}$$

where F_s is the required factor of safety.

The comparison of DLO analyses with those of Leshchinsky and Smith given in Figure 8 show close agreement, with DLO generally able to identify a more critical case as would be expected, since it is not restricted to one single failure mode. However the specific mechanism utilised Leshchinsky and Smith outperformed the DLO analysis marginally in two of the cases considered. This is not unexpected for circumstances where their mechanism closely matches the exact solution.

Figure 9 compares results of the DLO and the log-spiral limit analysis of Leshchinsky (1987) for a stability of embankment over soft soil. Leshchinsky (1987) checked bearing failure and deep seated failure. The results of the study showed that DLO was able to identify a more critical failure mechanism for all the above modes and in addition for surface lateral sliding.

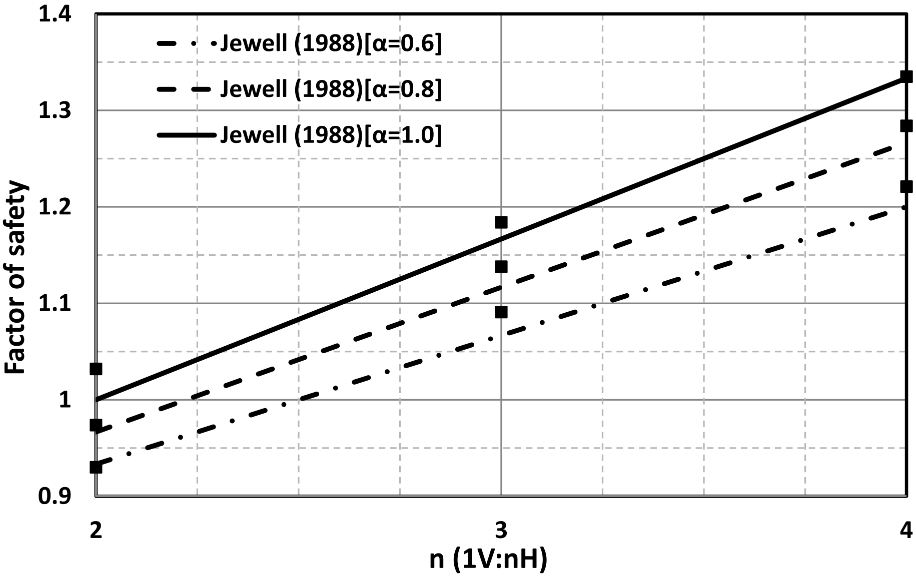

(a) Reinforced embankment over soft soil

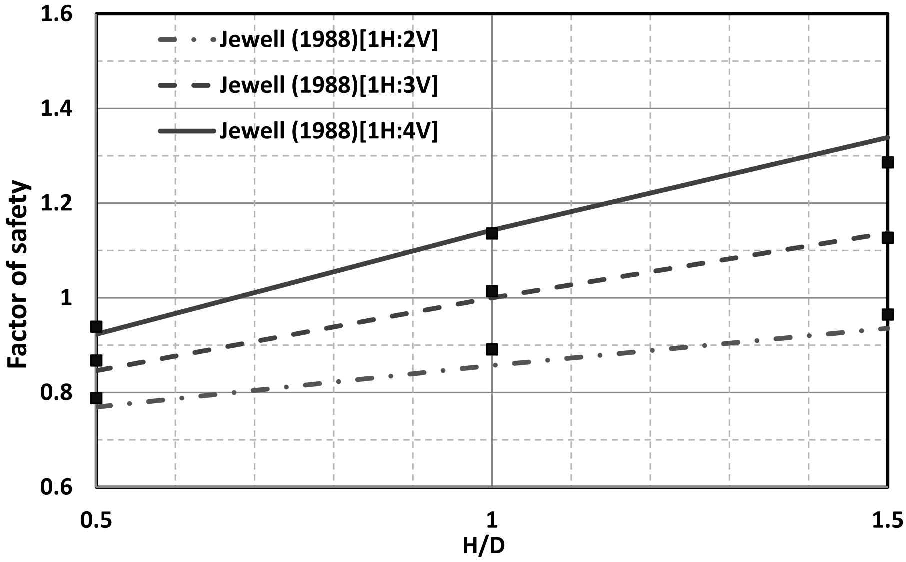

(b) Unreinforced embankment over soft soil

Figure 7: Plot of factor of safety against side slope gradient (n) for Jewell's analytical method (1988) and the current method (square markers) using parameters $c_u = 15\text{kPa}$, $\gamma = 18\text{kN/m}^3$, $\phi' = 30°$.

Hird (1986) produced a series of non-dimensional charts for cohesive and cohesionless reinforced embankments over soft soil using the limit equilibrium method of slices in which the reinforcement was modelled by applying a horizontal force to the sliding mass of soil. Figure 10 again shows good agreement, though since the work by Hird was based on Limit Equilibrium it is not possible to comment specifically on the relative magnitudes.

4.3.3. FE analysis

Rowe and Li (1999) and Rowe and Soderman (1987) investigated reinforced embankment problems by using finite element analysis. They investigated the required tensile stiffness of reinforcement (J: kN/m) for a given embankment height to achieve a factor of safety of one, and reported the maximum strain (ϵ_f) in the reinforcement at that point. A Limit Analysis method such as DLO cannot model elastic stiffness. Therefore to enable comparisons, the equivalent rupture strength R is calculated from the following equation:

$$R = J\epsilon_f \tag{6}$$

This limits the mobilised tensile stress in the reinforcement to the maximum value modelled in the FE analysis. However while in the FE model, this value represents the peak mobilised strength, possibly at one location only, in the DLO LA model, the mobilised strength is free to be distributed along the length of the reinforcement.

The model parameters investigated are given in Table 2. Figure 11 shows the corresponding maximum height H of the embankment for a variety of reinforcement rupture strengths. The results of the study shows that the FE method generally found more critical results (i.e. higher required rupture strengths) in comparison with DLO. This is attributed to the DLO model being able to redistribute the yield stress within the reinforcement, while the corresponding value in the FE model may only be a single peak value. However it is observed that this does not fully agree with the results of Tandjiria et al. (2002) who modelled the same scenarios using limit equilibrium and achieved closely similar results to the FE models with a range of different distributions of mobilised strength along the length of the reinforcement.

In summary the results show generally very good agreement with previous work, validating the DLO approach but also indicates that DLO is able to find more critical mechanisms in most cases.

5. Parametric study

5.1. Non-dimensional charts

The parametric study employed in this study investigated the geometry depicted in Figure 1 and the parameters given in Table 1. For a horizontal stratum of soil, the unit weight has no effect in undrained collapse, therefore the weight of the soft soil need not be considered. To efficiently cover a wide range of possible parameters, the study was conducted using the following 8 independent

Table 2: FE model comparison. Reinforced embankment analysis parameters. The undrained strength c_u varies linearly with depth z below the soft soil surface.

Parameter	**Embankment 1 (Rowe and Soderman, 1987)**	**Embankment 2 (Rowe and Li, 1999)**
W	30m	27m
n	2	2
ϕ'	32^o	37^o
γ	20 kN/m^3	20 kN/m^3
c_u (z=0m)	10kN/m^2	5.0kN/m^2
c_u (z=15m)	40kN/m^2	27.5kN/m^2
D	15m	15m
α_c	1.0	1.0
α_s	1.0	1.0

non-dimensional groups:

$$c'/\gamma H,\ c_u/\gamma H,\ R/\gamma H^2,\ q/\gamma H,\ H/D,\ n,\ \alpha \text{ and } \phi'$$

H was chosen as a normalising parameter for the first four groups since an increase in height of the embankment is expected to have the most significant effect on the stability. It was assumed that the embankment was sufficiently wide to avoid the collapse mechanism involving the centre. Based on the numerical model results, minimum values of W/D of approximately $4 + 2H/D$ are required for this assumption to hold true for most typical parameter sets. A comprehensive set of 72 charts were generated and are available in Electronic Annex 1 in the online version of this article. Different charts are presented for different values of:

- surcharge $q/\gamma H$ (0.0, 0.1),
- Interface coefficient α (0.6, 0.8, 1.0),
- Ratio of height of embankment and thickness of soft soil H/D (0.5, 1.0, 1.5),
- Angle of side slope 1V:nH (2, 3, 4),
- Low or high rupture strength of reinforcement $R/\gamma H^2$ (0.1, 1.0).

An example non-dimensional chart is presented in Figure 12 in terms of ϕ' vs $c_u/\gamma H$ for a range of values of $c'/\gamma H$. All graphs show the same qualitative pattern.

According to FHWA-NHI-00-043 (2001) the normal interface factor for geogrid and geotextiles varies between 0.6 and 0.8 respectively. In most design

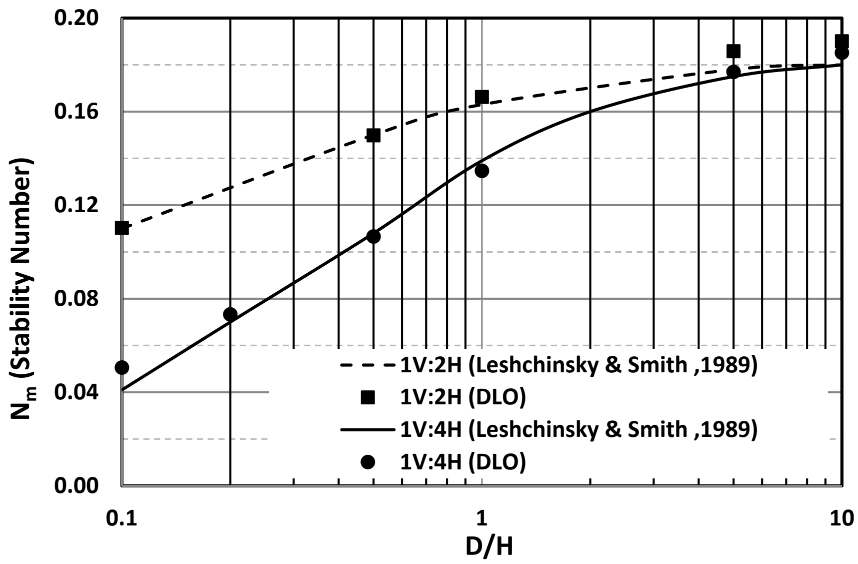

Figure 8: Comparison the result of DLO & Leshchinsky and Smith (1989) for an unreinforced embankment over soft soil. ($\phi' = 30°$)

guidelines and work examples, the interface coefficient for both top and bottom surfaces of the reinforcement is selected to be the same which has been done in this paper. Therefore the stated three interface coefficient values were modelled: 0.6, 0.8 and 1.0. It was necessary to model this only for the high rupture strength reinforcement because the dominant failure mechanism for weak reinforcement is global failure which is insignificantly affected by the shear resistance generated between the soil and geotextile. These parameters cover most typical embankments which are constructed over soft soil. Due to the symmetry of the model, only half of the cross-section was analysed with a symmetry boundary at one edge.

The maximum stable slope angle of a granular material is fundamentally related to the friction angle of the soil. Therefore, an embankment with zero cohesion and angle of friction less than the side slope angle is unstable. In this study, in order to extend the non dimensional graphs in this area, a small value of c' (equal to 0.1kPa) was set throughout the soil body to avoid local slope instability failure. Where this is done, it is indicated by a dashed line. Finally, for the design charts for the embankment with surcharge, there is no stable solution for a zero value of c' hence these are omitted from the charts.

5.2. Reinforcement strength

Two values of $R/\gamma H^2$ were employed in the generic parametric study, 0.1 and 1.0. This was intended to cover a broad range from very weak reinforcement (0.1) and strong reinforcement (1.0). To investigate the effect of reinforcement

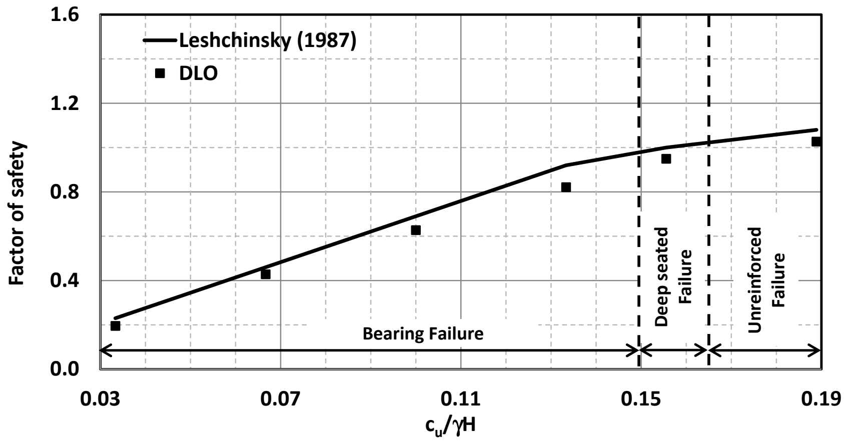

(a) H/D=0.1

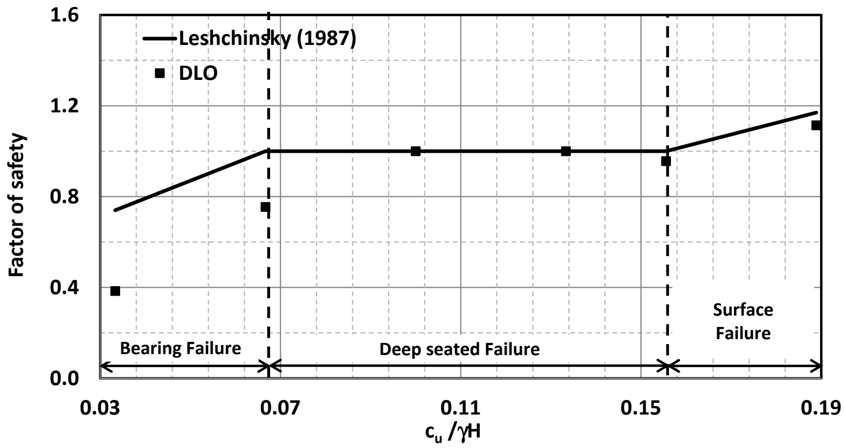

(b) H/D=1.0

Figure 9: Comparison of DLO and Leshchinsky (1987) for an embankment with slope 1V:2H over soft soil for ϕ'=30°. The factor of safety was on the shear strength of the soil. The mechanism description is based on the DLO analysis.

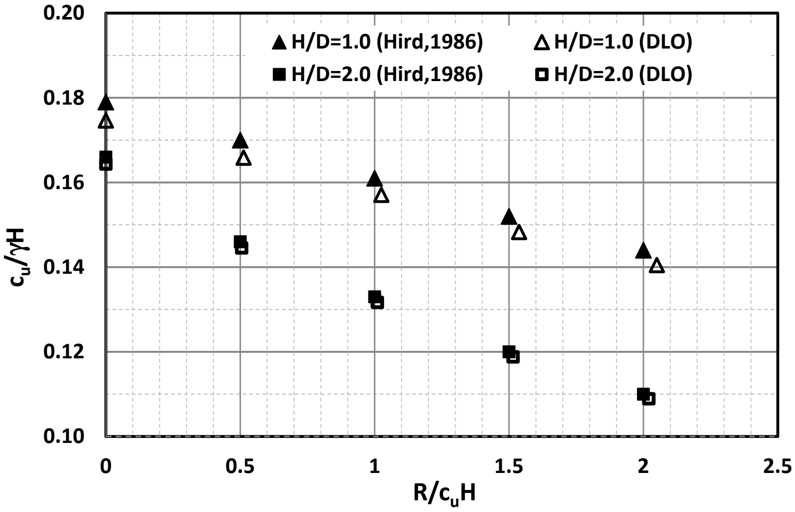

Figure 10: Plot of normalised undrained shear strength of soft soil required for stability against normalised reinforcement resistance for current method and Hird (1986). ($1V : 1.75H$, H=5m, γ=18kN/m^3, ϕ'=30°)

on stability, specific studies were also undertaken over a broad range of values of $R/\gamma H^2$. Figures 13a and b show how $c_u/\gamma H$ varies with reinforcement strength $R/\gamma H^2$ for a specific parameter set (H/D = 0.5, 1V:2H, c' = 0 and α = 0.8). It can be seen that for the no surcharge case, the solutions are independent of $R/\gamma H^2 > 1.0$ (this value will be defined as the limiting value $R_L/\gamma H^2$, at which the embankment will be said to be fully reinforced), and that there is a generally linear relationship between the parameters between $R/\gamma H^2$=0 to 0.7. Therefore if it is necessary to interpolate for R, a conservative approximation is to linearly interpolate between the values of R = 0 to R_L. An example interpolation is indicated in Figure 13b. In order to ensure conservative results, it can be seen that there will be a small error in the interpolation which is maximum between around $0.5R_L$ to $0.6R_L$. This maximum error is around 8% in c_u or around 20% in R. Further examples of the bilinear fit for a number of different parameter sets are reported in Electronic Annex 1 in the online version of this article and show similar behaviour.

Furthermore it can be seen that $R/\gamma H^2$ is very sensitive to changes in $c_u/\gamma H$, for values of $R < R_L$. Ideally the reinforcement should be designed from the horizontal portion of the curves (i.e. using R_L) and in design it would be preferable to apply a (partial) factor of safety to c_u rather than to R, or to both.

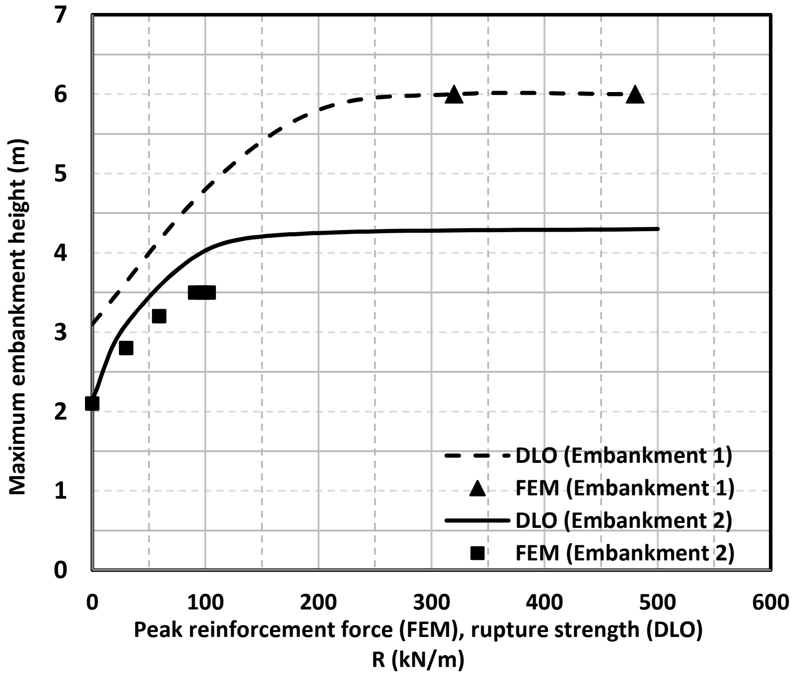

Figure 11: Comparison of the maximum height H of embankment versus reinforcement rupture strength R for current method, and peak reinforcement force for Rowe and Soderman, 1987 (Embankment 1) and Rowe and Li, 1999 (Embankment 2). Model parameters are given in Table 2.

5.3. Simplified design envelopes

It can be seen from the preceding graphs that the design region between fully stable or fully unstable embankments is relatively small in terms of the values of $c_u/\gamma H$. For example in Figure 13(b), independent of the value of $R/\gamma H^2$, and assuming that $\phi^{'} = 30^o$ always, the system will always be stable for $c_u/\gamma H > 0.176$ and always unstable for $c_u/\gamma H < 0.125$. Variants in the value of $\phi^{'}$ would change these values only by around 10% for failure modes where failure in the soft soil layer dominates. Other graphs e.g. Figure 12 show that additionally $c'/\gamma H$ also has a small effect (<10% on the value of $c_u/\gamma H$).

It is thus possible to plot a simplified design envelope of $c_u/\gamma D$ vs H/D for $\alpha = 0.8$, shown in Figure 14(a) for $\phi^{'} = 30^o$ and $c'/\gamma H = 0.0$ and Figure 14(b) for $\phi^{'} = 50^o$ and $c'/\gamma H = 0.1$. Two curves are given. Above the upper value the system is always stable (this corresponds to $R = 0$). Below the lower limit, it is generally always unstable (though minor gains may be made with stronger fill) and this corresponds to $R = R_L$. Values of $R_L/\gamma D^2$ are given on the same graph. In between the values the more detailed design charts

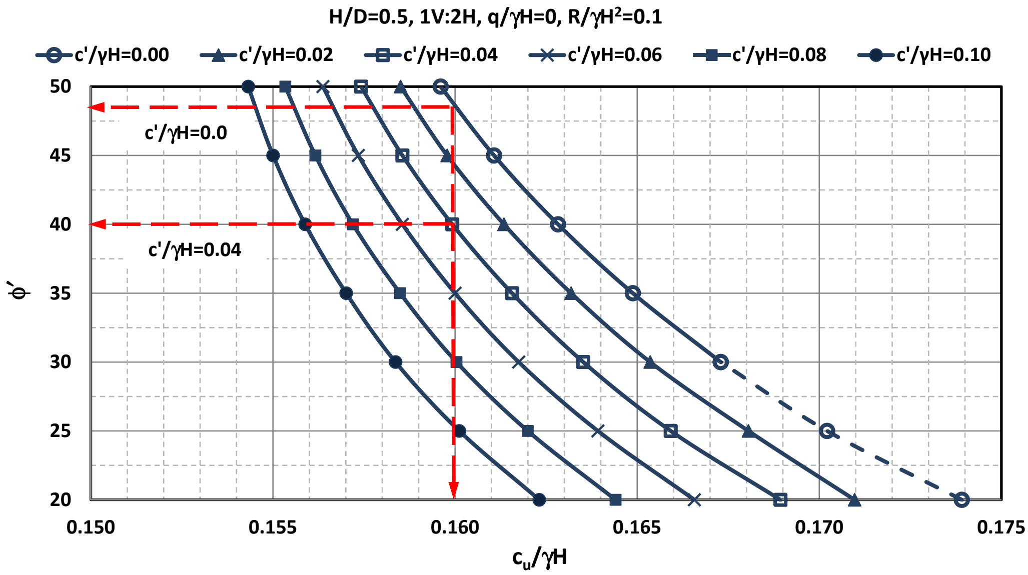

Figure 12: Value of ϕ' required for stability vs $c_u/\gamma H$ for $H/D = 0.5$, $n = 2$, $q = 0$ and $R/\gamma H^2 = 0.1$. This illustrates the type of graph generated from the parametric study discussed in Section 5. The long-dashed lines illustrate the design example presented in Section 6. A further 72 graphs are available in Electronic Annex 1 in the online version of this article.

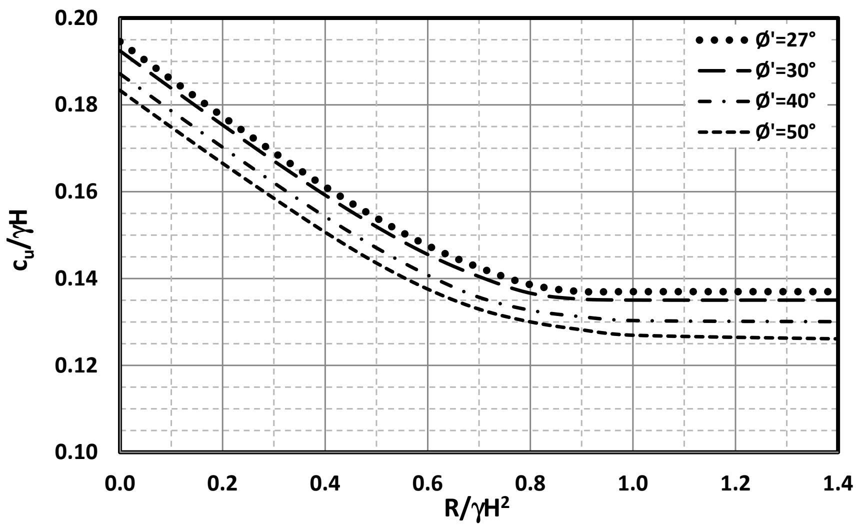

(a) With surcharge, $q/\gamma H = 0.1$

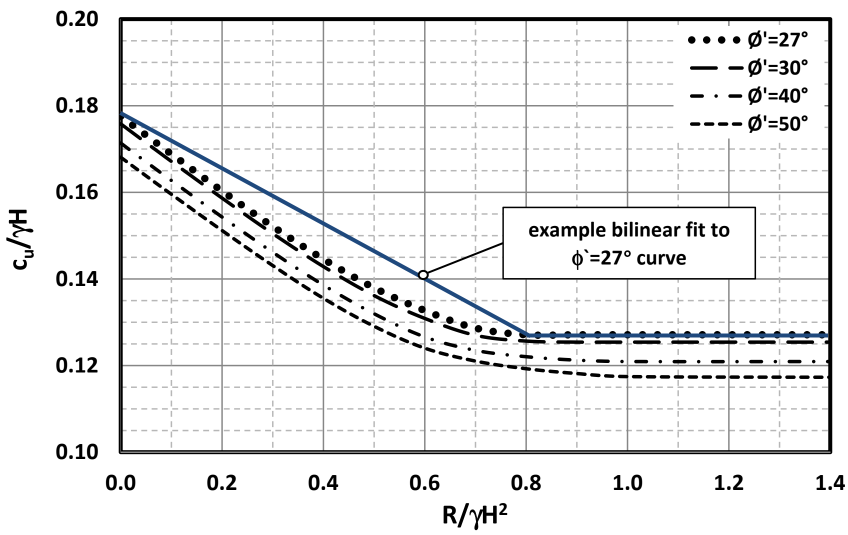

(b) Without surcharge

Figure 13: Required undrained shear strength for stability plotted against reinforcement strength($H/D = 0.5$, 1V:2H, $c' = 0$ and $\alpha = 0.8$).

must be used, or, as discussed previously, a linear interpolation can be used to provide a good estimate of R. Note that for these graphs the values of c_u and R_L have been normalised using D rather than H since this is expected to be an independent variable. Overall it can be seen that the use of reinforcement allows an embankment of a given size to be constructed on soft soil of around 50-100% the strength of that on which an unreinforced embankment could be constructed, depending on the value of H/D. It can also be seen that stronger fill has a marginal effect on the performance of a reinforced embankment, but a more significant effect on the stability of an unreinforced embankment.

Figure 14(b) also indicates that, for this example, an almost unlimited height of a fully reinforced embankment is possible for $c_u/\gamma D > \sim 0.16$ which may seem paradoxical, however this arises because the mechanism of failure is squeezing of the (relatively thin) confined soft soil layer which occurs over a width that extends beyond the embankment crest. Since the side slope width increases in tandem with the height, the bearing resistance in the soft soil layer also increases. It is noted that the reinforcement strength must also increase significantly with the height.

Finally Figure 15 shows that the limit equilibrium approach recommended by Jewell (1988), for extrusion only, provides a generally good fit to the data and is only slightly conservative compared with the current results for a fully reinforced embankment. The values it recommends involve an approximately 20% higher value of $c_u/\gamma D$ for a given H/D, but an approximately 10% smaller value of $R_L/\gamma D^2$. In combination this should still give a stable state but is slightly overconservative. To confirm this the interpolation method discussed in Section 5.2 was used on the Jewell value of $c_u/\gamma D$ to predict the corresponding required reinforcement strength $R/\gamma D^2$ using the current method. It can be seen that a value lower than the Jewell value of $R/\gamma D^2$ is predicted.

However, it is suggested that it would be preferable to design with the value of R_L to avoid the sensitivity to c_u discussed previously. It would also be expected that the extrusion equations would become less valid for values of $H/D < 0.25$, as a deep seated failure mode becomes more dominant.

6. Design example

Consider an embankment of 5m height and side slope $1H : 2V$ constructed from a coarse grained material of unit weight 17.5kN/m^3 overlying 10m of soft soil of uniform shear strength $c_u = 14kPa$ as shown in Figure 16. The required soil strength for the embankment fill when using a low rupture strength reinforcement (with $\alpha = 0.8$) without surcharge is determined as follows.

From Figure 14(a), it can be seen that design point D_1 plots at (H/D, $c_u/\gamma D$) = (0.5, 0.08) and that this lies between the maximum and minimum curves. In order to estimate the required reinforcement strength, the value $R_L/\gamma D^2 = 0.20$ can be read off the same graph (point R_1) for $H/D = 0.5$. This reinforcement strength is sufficient to support an embankment on a soil with $c_u/\gamma D = 0.063$. It is then possible to interpolate as follows:

Taking $c_{u,min}/\gamma D = 0.063$, $c_{u,max}/\gamma D = 0.089$, and $R_L/\gamma D^2 = 0.20$.

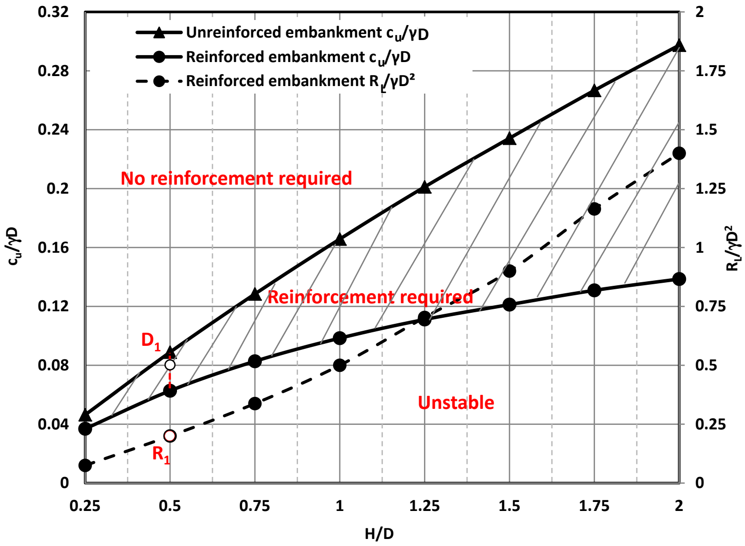

(a) $\phi' = 30°$, $c' = 0$

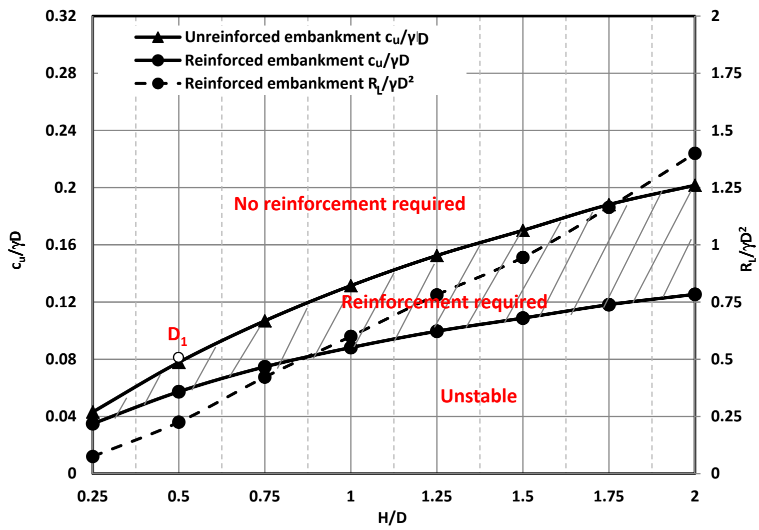

(b) $\phi' = 50°$, $\frac{c'}{\gamma H} = 0.1$

Figure 14: Simplified design domains ($\alpha = 0.8$, $q = 0$ and $n = 2$). The reinforced embankment case uses reinforcement with rupture strength R_L the value of which is given in the same plot. The shaded zone is the design domain where reinforcement is required. Below this zone stability is not possible with a single layer of reinforcement.

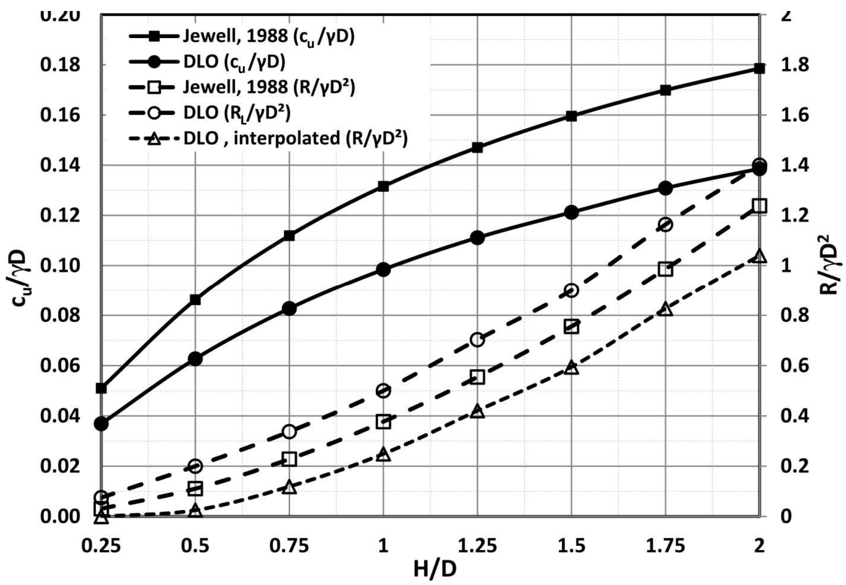

Figure 15: Comparison of results from the current method and Jewell (1988), equations 2 and 3, for determining the required shear strength of soft soil and rupture strength of reinforcement for stability $\phi' = 30°$, $c' = 0$, $\alpha = 0.8$, $q = 0$ and $n = 2$). The 'interpolated' line shows the predicted required value of $R/\gamma D^2$ using the current method based on the value of c_u specified by the method of Jewell.

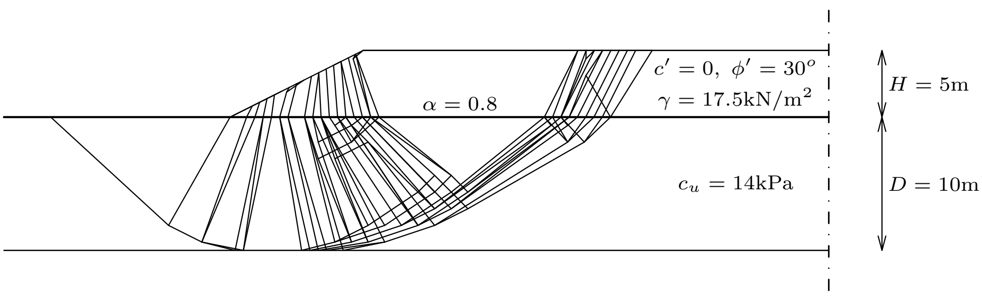

Figure 16: Design example geometry and failure mechanism associated with the determined geotextile rupture strength $R = 121$ kN/m.

$$\frac{R}{\gamma D^2} = \frac{R_L}{\gamma D^2}\frac{c_{u,max} - c_u}{c_{u,max} - c_{u,min}} = 0.20\frac{0.089 - 0.08}{0.089 - 0.063} = 0.069 \quad (7)$$

Hence the required reinforcement tensile strength R is 121 kN/m. This result is valid for embankment fill of $\phi' = 30^o$ and $c' = 0$ and will be slightly overconservative due to the linear interpolation approximation. For a stronger fill of $\phi' = 50^o$ and $c' = 0.1\gamma H = 8.8$ kN/m^2, Figure 14(b) indicates that no reinforcement is required.

As noted before R has a significant degree of sensitivity to $c_u/\gamma H$, e.g. a reduction in c_u of 10% can lead to a change in R of 60%. However a reduction in c_u of 15% will lead to a situation that cannot be stabilised by reinforcement. For a more detailed study, the case of $R/\gamma H^2 = 0.1$ can be investigated using the charts presented in Electronic Annex 1 in the online version of this article. The graph therefore corresponds to a model where the reinforcement rupture strength is a low value of $R = 44$ kN/m. In this case failure is typically by reinforcement rupture, combined with soil failure.

First the relevant chart is chosen (shown also in Figure 12) based on the values of $H/D = 0.5$, slope $1H : 2V$, and $q/\gamma H = 0$. Having selected the graph, the x-axis can be read off using $c_u/\gamma H = 0.16$. A family of curves then allows different combinations of c' and ϕ' to be selected such as ($c' = 0, \phi' = 48^o$) or ($c'/\gamma H = 0.04$, ie $c' = 3.5$ kPa, $\phi' = 40^o$) which is the required shear strength of the embankment soil for a factor of safety of 1.0. This is consistent with the previous result that indicated that reinforcement was not necessary for $\phi' = 50^o$. If higher factors of safety are required then these can be applied as appropriate to the parameters.

7. Discussion

The validation studies indicate that the factor of safety computed with the DLO method is typically lower than the conventional limit analysis and limit equilibrium methods. This is due to the critical failure mechanism not being pre-defined. However the DLO results were slightly above those given by the FE analyses of Rowe and Li (1999) and Rowe and Soderman (1987). The reasons for this are not clear but it may be related to the nature of the Limit Analysis approach. The results presented are strictly only valid within this framework which essentially assumes that the soil and reinforcement are rigid-plastic materials. At failure the material must either have not yielded or if it has yielded, it must display a fully ductile plastic response with constant resistance at any strain level.

In practice many geotextiles do display this type of response and so it would be reasonable to assume that soil and geotextile can reach full strength at compatible strain levels at failure. It would be necessary to check that the the limit analysis results indicate reasonably uniform elongation rates along the length of the failing zone, so that high concentrations of strain are not anticipated.

For geotextiles that would rupture rather than stretch at a relatively low strain level, then their (suitably factored) strength should be chosen to be greater than the limiting value R_L. For such cases it is observed that the interface coefficients α_c and α_s do influence the results (by $\sim 10\%$), whereas below this value the reinforcement will tend to yield before the shear strength on the interface is reached, thus rendering the value of α less significant (as long as it is reasonably large).

8. Conclusions

1. The DLO analysis has been shown to find more critical failure mechanisms compared with other limit equilibrium results in the literature for most cases. It was also able to identify a previously unreported bearing type failure mechanism which involves rotational 'snapping' of the embankment.
2. The use of reinforcement allows an embankment of a given height H to be constructed on a depth D of soft soil of around 50-100% the strength of that on which an unreinforced embankment could be constructed, depending on the value of H/D. Use of very strong compared to lower strength embankment fill has only a marginal additional effect of allowing construction on a soft soil of around 10% lower strength.
3. Design charts have been presented that can be used for determining the maximum stable height and required reinforcement strength for fully reinforced (where the reinforcement is not taken to yield) and unreinforced embankments resting over soft soil and the transition between these two states which is shown to result in an approximately linear relationship between the required reinforcement rupture strength and the undrained shear strength of the soft soil.
4. It is recommended that embankments be designed at the point where the reinforcement is not taken to yield to avoid an observed sensitivity to the soft soil strength for cases where reinforcement and soil yield together.

Appendix

Appendix A. Precision of DLO solution

FigureA.1 shows the factor of safety on soil strength versus the number of nodes across embankment height. A value of 5 nodes across the embankment height provides an accuracy of 1-2%.

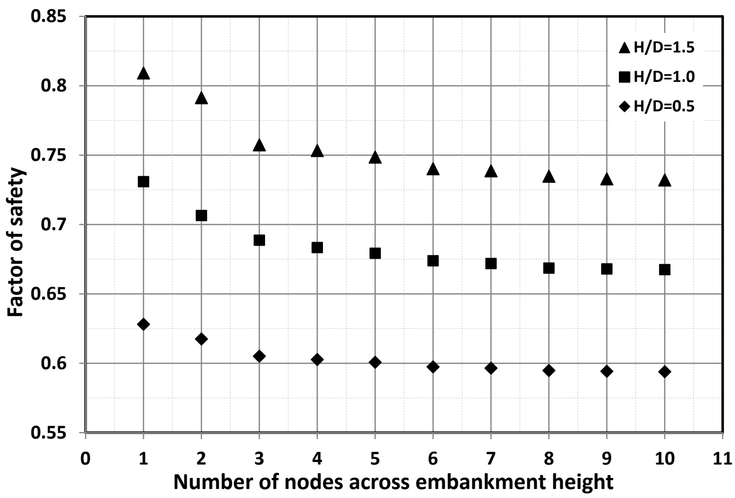

Figure A.1: Variation of factor of safety versus DLO nodal spacing

References

Chai, J.C., Bergado, D., 1993. Some techniques for finite element analysis of embankments on soft ground. Canadian Geotechnical Journal 30, 710–719.

Clarke, S., Smith, C., Gilbert, M., 2013. Modelling discrete soil reinforcement in numerical limit analysis. Canadian Geotechnical Journal 50, 705–715.

Duncan, J., 1996. State of the art: Limit equilibrium and finite-element analysis of slopes. Journal of Geotechnical Engineering 122, 557–596.

Duncan, J.M., Buchignani, A.L., De Wet, M., 1987. An engineering manual for slope. Virginia Polytechnic Institute and State University Reproduced by the University of Wisconsin-Madison with permission and courtesy of the Virginia Polytechnic Institute and State University.

Duncan, J.M., Schaefer, V.R., 1988. Finite element consolidation analysis of embankments. Computers and Geotechnics 6, 77–93.

FHWA-NHI-00-043, 2001. Mechanically stabilized earth walls and reinforced soil slopes, Design & Construction Guidelines. U.S. Department of Transportation Federal Highway Administration.

Gilbert, M., Smith, C., Haslam, I., Pritchard, T., 2010. Application of discontinuity layout optimization to geotechnical engineering, pp. 169–174. Proceedings of the 7th European Conference on Numerical Methods in Geotechnical Engineering.

Hird, C.C., 1986. Stability charts for reinforced embankment on soft ground. Geotextiles and Geomembranes 4, 107–127.

Hird, C.C., Kwok, C.M., 1989. Finite element studies of interface behaviour in reinforced embankments of soft ground. Computers and Geotechnics 8, 111–131.

Hird, C.C., Pyrah, I.C., Russell, D., 1990. Finite element analysis of the collapse of reinforced embankments on soft ground. Geotechnique 40, 633–640.

Jewell, R.A., 1988. The mechanics of reinforced embankment on soft soils. Geotextiles and Geomembranes 7, 237–273.

Jewell, R.A., 1996. Soil reinforcement with geotextile. London: Construction Industry Research and Information Association.

Leshchinsky, B., 2015. Bearing capacity of footings placed adjacent to c'-ϕ' slopes. Journal of Geotechnical and Geoenvironmental Engineering 141, 04015022.

Leshchinsky, D., 1987. Short-term stability of reinforced embankment over clayey. Soil and Foundation 29, 105–114.

Leshchinsky, D., Smith, D.S., 1989. Deep seated failure of a granular embankment over clay: Stability analysis. Soil and Foundation 27, 43–57.

Leshchinsky, D., Vahedifard, F., Leshchinsky, B.A., 2012. Revisiting bearing capacity analysis of MSE walls. Geotextiles and Geomembranes 34, 100–107.

LimitState, 2014. LimitState:GEO Manual Version 3.2.a. june 2014 ed. LimitState Ltd.

Manceau, S., Macdiarmid, C., Horgan, G., 2012. Design of soil reinforced slopes and structures, in: Burland, J., Chapman, T., Skinner, H., Brown, M. (Eds.), ICE manual of geotechnical engineering, Volume II geotechnical design, Construction and verification., pp. 1093–1107.

Rowe, R., Li, A.L., 2005. Geosynthetic-reinforced embankments over soft foundation. Geosynthetics International 12, 50–85.

Rowe, R.K., Hinchberger, S.D., 1998. The significance of rate effects in modelling the sackville test embankment. Canadian Geotechnical Journal 35, 500–516.

Rowe, R.K., Li, A.L., 1999. Reinforced embankment over soft foundations under undrained and partially drained conditions. Geotextiles and Geomembranes 17, 129–146.

Rowe, R.K., Soderman, K., 1987. Stabilization of very soft soils using high strength geosynthetics: the role of finite element analyses. Geotextiles and Geomembranes 6, 53–80.

Rowe, R.K., Soderman, K.L., 1985. An approximate method for estimating the stability of geotextile-reinforced. Canadian Geotechnical Journal 22, 392–398.

Sabhahit, N., Basudhar, P.K., Madhav, M.R., Miura, N., 1994. Generalized stability analysis of reinforced embankment on soft clay. Geotextiles and Geomembranes 13, 765–780.

Smith, C., Gilbert, M., 2007. Application of discontinuity layout optimization to plane plasticity problems. Royal Society A: Mathematical, Physical and Engineering Sciences 463, 2461–2484.

Smith, C.C., Gilbert, M., 2013. Identification of rotational failure mechanisms in cohesive media using discontinuity layout optimisation. Geotechnique 63, 1194–1208.

Tandjiria, V., Low, B.K., Teh, C.I., 2002. Effect of reinforcement force distribution on stability of embankments. Geotextiles and Geomembranes 20, 423–443.

Vahedifard, F., Leshchinsky, B.A., Sehat, S., Leshchinsky, D., 2014. Impact of cohesion on seismic design of geosynthetic-reinforced earth structures. Journal of Geotechnical and Geoenvironmental Engineering 140, 04014016.

Zhang, N., Shen, S.L., Wu, H.N., Chai, J.C., Xu, Y.S., Yin, Z.Y., 2015. Evaluation of effect of basal geotextile reinforcement under embankment loading on soft marine deposits. Geotextiles and Geomembranes 43, 506 – 514. Special issue on Soft Ground Improvement using Geosynthetics Applications.